

This paper is published as part of a *Dalton Transactions* themed issue on:

## The Synergy between Theory and Experiment

Guest Editor John McGrady  
University of Glasgow, UK

Published in [issue 30, 2009](#) of *Dalton Transactions*

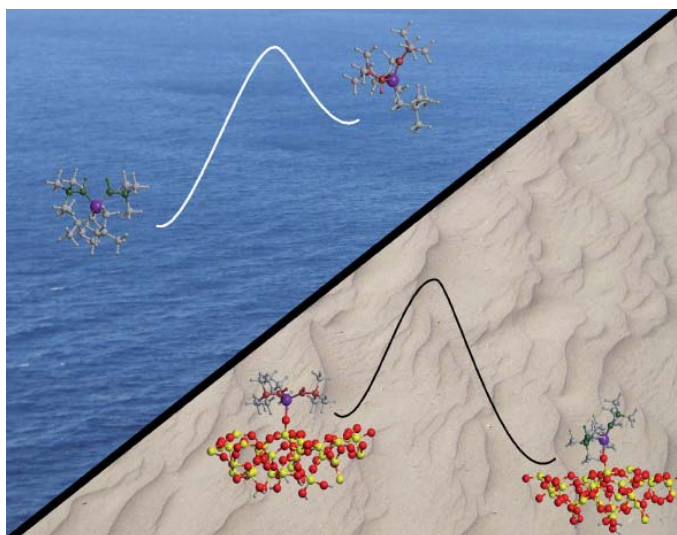


Image reproduced with permission of Christophe Coperet

Papers published in this issue include:

[A combined picture from theory and experiments on water oxidation, oxygen reduction and proton pumping](#)

Per E. M. Siegbahn and Margareta R. A. Blomberg, *Dalton Trans.*, 2009,  
DOI: [10.1039/b903007g](#)

[Mechanisms of C–H bond activation: rich synergy between computation and experiment](#)

Youcef Boutadla, David L. Davies, Stuart A. Macgregor and Amalia I. Poblador-Bahamonde,  
*Dalton Trans.*, 2009,  
DOI: [10.1039/b904967c](#)

[Are tetrathiooxalate and diborinate bridged compounds related to oxalate bridged quadruply bonded compounds of molybdenum?](#)

Malcolm H. Chisholm and Namrata Singh, *Dalton Trans.*, 2009  
DOI: [10.1039/b901734h](#)

[Molecular recognition in Mn-catalyzed C–H oxidation. Reaction mechanism and origin of selectivity from a DFT perspective](#)

David Balcells, Pamela Moles, James D. Blakemore, Christophe Raynaud, Gary W. Brudvig, Robert H. Crabtree and Odile Eisenstein, *Dalton Trans.*, 2009  
DOI: [10.1039/b905317d](#)

Visit the *Dalton Transactions* website for more cutting-edge inorganic and organometallic research  
[www.rsc.org/dalton](http://www.rsc.org/dalton)

# Aromatic C–F activation by complexes containing the {Pt<sub>2</sub>S<sub>2</sub>} core *via* nucleophilic substitution: a combined experimental and theoretical study†

Ainara Nova,<sup>a</sup> Rubén Mas-Ballesté,<sup>a,b</sup> Gregori Ujaque,<sup>a</sup> Pilar González-Duarte<sup>\*a</sup> and Agustí Lledós<sup>\*a</sup>

Received 26th January 2009, Accepted 13th May 2009

First published as an Advance Article on the web 27th May 2009

DOI: 10.1039/b901697j

The C–F bond activation of perfluorobenzene and perfluoropyridine have been achieved by means of the complex [Pt<sub>2</sub>(μ-S)<sub>2</sub>(dppp)<sub>2</sub>], where dppp denotes 1,3-bis(diphenylphosphino)propane. The reaction with the first substrate requires a long time (five days) and high temperature (reflux in toluene) to yield [Pt(*o*-S<sub>2</sub>C<sub>6</sub>F<sub>4</sub>)(dppp)] and [Pt<sub>3</sub>(μ<sub>3</sub>-S)<sub>2</sub>(dppp)<sub>3</sub>]F<sub>2</sub>, and involves replacement of two fluorides in the *ortho* position. In contrast, the reaction with perfluoropyridine is much faster (15 min at 0 °C) yielding [Pt<sub>2</sub>(μ-S){μ-(*p*-SC<sub>5</sub>F<sub>4</sub>N)}(dppp)<sub>2</sub>]F, which implies the C–F activation in the *para* position with respect to the pyridine nitrogen. The mechanism of both reactions has been studied computationally and the geometries of the transition states are consistent with an S<sub>N</sub>Ar mechanism where a sulfido bridging ligand replaces the fluoride anion. The energy barriers corresponding to the first and the second fluoride substitution are 131.7 and 137.1 kJ mol<sup>-1</sup> for perfluorobenzene and 85.9 and 142.7 kJ mol<sup>-1</sup> for perfluoropyridine, respectively. The different energy barrier of the first substitution explains the different experimental conditions required and the various products obtained for these reactions.

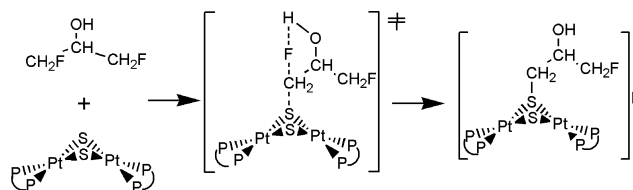
## Introduction

Organofluorine chemistry is an active field of research due to the interesting properties that fluorine furnishes to the carbon skeleton.<sup>1</sup> As a consequence, these compounds show a great variety of uses in the pharmaceutical industry and in material science.<sup>2</sup> One strategy to synthesize organofluorine derivatives is the functionalization of polyfluorinated organic compounds. Two main different routes to achieve this goal have been widely explored: (1) C–F bond activation at transition metal centers,<sup>3–8</sup> and (2) nucleophilic substitution of the fluoride anion by organic nucleophiles.<sup>9,10</sup> The advantages of the former strategy are the selectivity of the reactions and the catalytic role of metallic centers.<sup>11–14</sup> However, the reluctance of C–F bonds to undergo oxidative additions with a metal centre and possible C–H activation as a competitive reaction are important drawbacks.<sup>4,15,16</sup> Concerning the second strategy, the C–F bond is often the easiest C–halogen bond to be activated by nucleophilic aromatic substitution (addition + elimination) as a consequence of the major polarity of this bond that facilitates the addition step, which usually is the rate-determining step.<sup>10</sup> This mechanism takes place in reactions with organic nucleophiles such as sulfur, oxygen and nitrogen-based systems.<sup>10</sup> However, controlling the selectivity using organic nucleophiles is a main challenge because the control of the number of fluorine atoms to be activated is

not obvious.<sup>9,10</sup> In addition, it has been reported intramolecular C–F bond activation on the coordination sphere of metallic centres by the nucleophilic attack of coordinated ligands such as H<sub>2</sub>O,<sup>17</sup> OH,<sup>18</sup> SH<sub>2</sub><sup>19</sup> or NEt<sub>3</sub>.<sup>20</sup> A novel mechanism involving nucleophilic attack of an electron-rich organometallic compound and trapping of the displaced fluoride by a phosphine ligand to form a metallophosphorane intermediate has been recently identified with the help of DFT calculations.<sup>21–23</sup> The strategy proposed herein is to confine the nucleophilic group between two metal centres, which will direct selective activation of only one or two C–F bonds of aromatic perfluorinated compounds.

Within this context, the reactivity of the {Pt<sub>2</sub>S<sub>2</sub>} core in [L<sub>2</sub>Pt(m-S)<sub>2</sub>PtL<sub>2</sub>] compounds with organic electrophiles becomes specially attractive.<sup>24,25</sup> It has been reported over the last decade that sulfur atoms in the {Pt<sub>2</sub>S<sub>2</sub>} core are highly nucleophilic and, as a consequence, C–X (X = Cl, Br, I) bonds can be activated.<sup>26–33</sup> Thus, it is possible to make use of the high nucleophilicity of the bridging sulfido ligand to achieve C–X activation by taking advantage of the metallic framework that solubilises the sulfide anion in organic solvents, modulates its reactivity and induces selectivity on the corresponding reactions.

Recently, the reaction of [Pt<sub>2</sub>(μ-S)<sub>2</sub>(dppp)<sub>2</sub>] (**I**) with 1,3-difluoro-2-propanol (Scheme 1) allowed us to provide the first example of C–F activation by the {Pt<sub>2</sub>S<sub>2</sub>} core.<sup>34</sup> The computational study



**Scheme 1** Reaction between [Pt<sub>2</sub>(μ-S)<sub>2</sub>(dppp)<sub>2</sub>] (**I**) and 1,3-difluoro-2-propanol.

<sup>a</sup>Departament de Química, Universitat Autònoma de Barcelona, 08193 Bellaterra, Barcelona, Catalonia, Spain. E-mail: agusti@klingon.uab.es, pilar.gonzalez.duarte@uab.es; Fax: +34-935812920; Tel: +34-935811363

<sup>b</sup>Departamento de Química Inorgánica, Universidad Autónoma de Madrid, 28049, Madrid, Spain

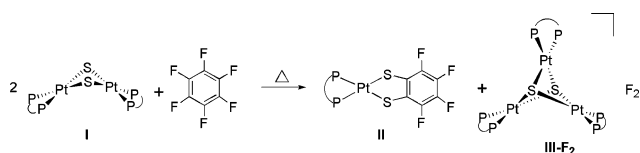
† Electronic supplementary information (ESI) available: <sup>31</sup>P{<sup>1</sup>H}, <sup>19</sup>F NMR and MS spectra. Energies and optimized geometries (Cartesian coordinates). CCDC reference numbers 717503 (**II**) and 717504 (**IV**). For ESI and crystallographic data in CIF or other electronic format see DOI: 10.1039/b901697j

of the reaction mechanisms showed that, in this reaction, the assistance of the OH group on the fluorine departure was a main factor to facilitate the Csp<sup>3</sup>-F bond activation. The reaction proceeds through a S<sub>N</sub>2 mechanism where the O-H...F hydrogen bond established from the alcohol group of the organic substrate is essential stabilizing the departure of the fluoride anion.<sup>34</sup> Extending our previous work, we have explored the reactivity of **I** with unsaturated substrates such as perfluorobenzene (pfb) and perfluoropyridine (pfp). Remarkably, the conditions required to achieve these reactions and the products obtained are substrate-dependent. Synergy between experiments and theory is illustrated in this work by the mechanistic insights obtained from DFT calculations, which complete our understanding of the reactions carried out in the laboratory.

## Results and discussion

### Double C-F bond activation in perfluorobenzene

**Experimental study.** Treatment of [Pt<sub>2</sub>(μ-S)<sub>2</sub>(dppp)<sub>2</sub>] (**I**) with an excess of perfluorobenzene in toluene at reflux for 5 days yielded two products: [Pt(*o*-S<sub>2</sub>C<sub>6</sub>F<sub>4</sub>)(dppp)] (**II**) and [Pt<sub>3</sub>(μ<sub>3</sub>-S)<sub>2</sub>(dppp)<sub>3</sub>]<sup>+2</sup>(F<sup>-</sup>)<sub>2</sub> (**III-F<sub>2</sub>**) (Scheme 2). The species present in the reaction mixture were monitored by <sup>31</sup>P{<sup>1</sup>H} NMR. The series of spectra recorded as a function of time indicated that **I** completely evolved into **II** without detection of any intermediate. While complex **II** is soluble in the reaction medium, complex **III-F<sub>2</sub>** is insoluble and was isolated by filtration. The formulation of **III-F<sub>2</sub>** as [Pt<sub>3</sub>(μ<sub>3</sub>-S)<sub>2</sub>(dppp)<sub>3</sub>]<sup>+2</sup>(F<sup>-</sup>)<sub>2</sub> was confirmed by <sup>31</sup>P-NMR measurements in d<sub>6</sub>-DMSO, which showed identical spectroscopic features than those obtained for complex [Pt<sub>3</sub>(μ<sub>3</sub>-S)<sub>2</sub>(dppp)<sub>3</sub>](PF<sub>6</sub>)<sub>2</sub>, whose synthesis, X-ray structure and NMR parameters have been previously reported.<sup>35</sup>



Complex **II**, which comes from the double C-F bond activation in perfluorobenzene, was isolated by evaporating to dryness the solution obtained after filtering off the solid product **III-F<sub>2</sub>**. **II** was characterized by NMR (<sup>31</sup>P{<sup>1</sup>H} and <sup>19</sup>F), FAB mass spectrometry and X-ray diffraction. The P{<sup>1</sup>H} NMR spectrum in d<sub>6</sub>-DMSO shows a set of signals centred at -5.37 ppm (*J*<sub>Pt-P</sub> = 2684 Hz) consistent with a complex with chemically equivalent phosphorus nuclei. The fine structure of the central signal discloses a triplet, which is consistent with the coupling of phosphorus with two equivalent F nuclei located at a distance of 5 bonds (*J*<sub>P-F</sub> = 6 Hz). This long distance coupling is also observed in the related [Os(SC<sub>6</sub>F<sub>5</sub>)<sub>2</sub>(S<sub>2</sub>C<sub>6</sub>F<sub>4</sub>)(PMe<sub>2</sub>Ph)] complex.<sup>36</sup> In the <sup>19</sup>F NMR of **II** only two signals appeared ( $\delta$  = 140.2 ppm; 167.4 ppm), which is consistent with the formation of a complex by activation of two C-F bonds in *ortho* position. Finally, the FAB MS spectrum, which showed a major peak at *m/z* = 820.7 Da, is also in agreement with the theoretical expected value for [Pt(*o*-S<sub>2</sub>C<sub>6</sub>F<sub>4</sub>)(dppp)]H<sup>+</sup> (820.1 Da).

**Table 1** Selected bond lengths (Å) and angles (°) for complex **II**

<b>II</b>			
Bond lengths/Å			
Pt(1)-P(1)	2.2638(14)	Pt(1)-S(2)	2.3044(13)
Pt(1)-P(2)	2.2691(14)	S(1)-C(1)	1.747(5)
Pt(1)-S(1)	2.3031(14)	S(2)-C(6)	1.727(6)
Bond angles/°			
P(1)-Pt(1)-P(2)	89.88(5)	P(2)-Pt(1)-S(2)	177.45(5)
P(1)-Pt(1)-S(1)	176.43(5)	S(1)-Pt(1)-S(2)	89.73(5)
P(2)-Pt(1)-S(1)	89.80(5)	C(1)-S(1)-Pt(1)	103.15(19)
P(1)-Pt(1)-S(2)	90.75(5)	C(6)-S(2)-Pt(1)	103.26(18)

X-Ray quality crystals were obtained by slow evaporation of a DMSO-acetone solution. The structure of complex **II**, depicted in Fig. 1, consists of mononuclear [Pt(*o*-S<sub>2</sub>C<sub>6</sub>F<sub>4</sub>)(dppp)] discrete molecules devoid of crystallographic symmetry elements. The listing of the main geometric parameters for **II** appears in Table 1. The structure can be considered as formed by two rings that share a platinum atom. One is an essentially planar five-membered PtS<sub>2</sub>C<sub>2</sub> ring (dihedral PtSCC angle of 3.6°), which has a common edge with the aromatic cycle of the chelating [*o*-S<sub>2</sub>C<sub>6</sub>F<sub>4</sub>]<sup>2-</sup> ligand. The other is the C<sub>3</sub>P<sub>2</sub>Pt ring that includes six atoms and shows a chair conformation. The platinum atom has square planar coordination, with a S-Pt-S angle of 89.73(5)°, very close to the ideal value of 90°. The bite angle of the diphosphine ligand, 89.88(5)°, dictates the values of the remaining P-Pt-S angles about the platinum atom (89.88(5)° and 90.75(5)°).

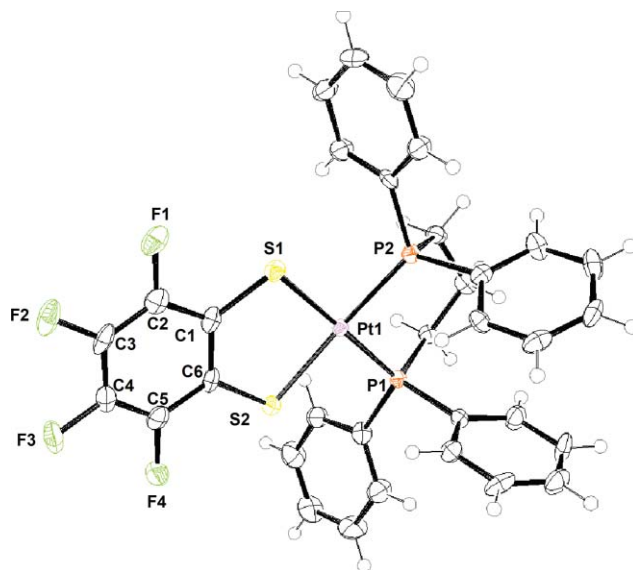


**Fig. 1** Displacement ellipsoid plot (20% probability) of [Pt(*o*-S<sub>2</sub>C<sub>6</sub>F<sub>4</sub>)(dppp)] (**II**). H atoms omitted.

**Theoretical study.** The theoretical study of the reaction of [Pt(μ-S)<sub>2</sub>(dppp)<sub>2</sub>] (**I**) with perfluorobenzene (pfb) has been performed using DFT methods. In this study the dppp ligands have been modelled by H<sub>2</sub>P(CH<sub>2</sub>)<sub>3</sub>PH<sub>2</sub> (dhpp). As shown in Fig. 2 and 3, this reaction initiates with the attack of the bridging sulfido ligand in [Pt(μ-S)<sub>2</sub>(dhpp)<sub>2</sub>] (**I**) to one of the carbon atoms of

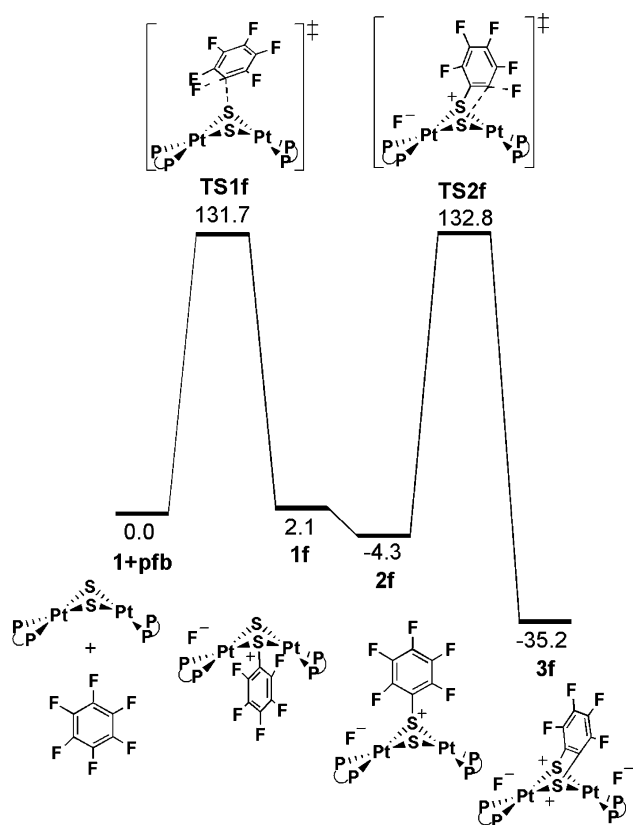


Fig. 2 Energy profile in toluene of the C–F bond activation mechanism of perfluorobenzene (pfb) by  $[\text{Pt}_2\text{S}_2(\text{dhpp})]$  (**1**). All energies in  $\text{kJ mol}^{-1}$ .

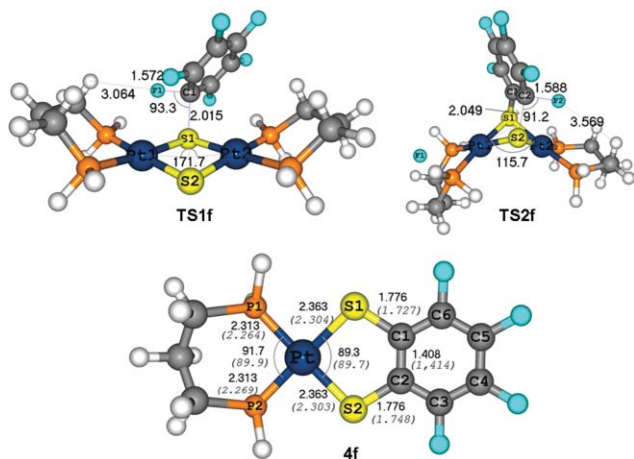


Fig. 3 Optimized geometries of transition states (**TS1f** and **TS2f**) and complex **4f** with the most representative distances ( $\text{\AA}$ ) calculated for this model structure and found in the crystal structure of **II** (numbers in italics).

perfluorobenzene and the concomitant departure of the fluoride ion in transition state **TS1f** ( $\text{S}\cdots\text{C} = 2.015 \text{ \AA}$  and  $\text{C}\cdots\text{F} = 1.572 \text{ \AA}$ ). In this transition state, the  $\{\text{Pt}_2\text{S}_2\}$  core is almost planar with a dihedral angle of  $171.7^\circ$  and an SCF angle of  $93.3^\circ$ . In this way the leaving fluoride is stabilized by interaction with the aliphatic chain of the phosphine (see Fig. 3). This geometry induces the product of this step, the ion pair **1f**, to have the  $\text{C}_6\text{F}_5$  group in endo position with respect to the  $\{\text{Pt}_2\text{S}_2\}$  core with a  $\text{P}\cdots\text{F}$  distance remarkably short ( $1.996 \text{ \AA}$ ) indicating a

strong interaction between both centres. The importance of this interaction in several C–F bond activation reactions has been already reported by Macgregor *et al.*<sup>21–23</sup> The energy barrier of this first fluoride substitution is  $131.7 \text{ kJ mol}^{-1}$  and the energy difference between reactant and product is  $2.1 \text{ kJ mol}^{-1}$  (Fig. 2). From **1f**, the direct second C–F bond activation is not possible and a previous endo–exo isomerisation is required. It has been shown that this process is usually easy for complexes containing the  $\{\text{Pt}_2\text{S}(\text{SR})\}$  core (*vide infra*).<sup>37–39</sup>

Intermediate **2f**, with  $\text{C}_6\text{F}_5$  group in exo position and perpendicular to the plane defined by SSC, is  $6.4 \text{ kJ mol}^{-1}$  more stable than the endo isomer. From this intermediate it takes place the substitution of the second fluoride anion in *ortho* position through **TS2f** ( $\text{S}\cdots\text{C} = 2.049 \text{ \AA}$  and  $\text{C}\cdots\text{F} = 1.588 \text{ \AA}$ ) with an energy barrier of  $137.1 \text{ kJ mol}^{-1}$  (Fig. 2 and 3). The dihedral angle of the  $\{\text{Pt}_2\text{S}_2\}$  core in this transition state is  $115.7^\circ$  and the SCF angle  $91.2^\circ$ . In this case, the fluoride departure occurs in the direction opposite to the first one. By this way, the fluoride ion can be better stabilized by the other dhpp phosphine. The product of the second substitution is **3f**, an ion pair where the group  $\text{S}_2\text{C}_6\text{F}_4$  is bridging the two Pt atoms. This species is  $35.2 \text{ kJ mol}^{-1}$  more stable than the reactants, which makes the reaction to be exothermic.

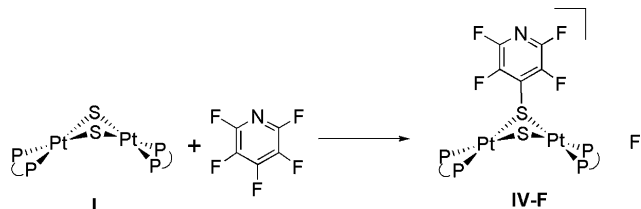
The next step of the reaction to obtain product **II** is the fragmentation of **3f** to give  $[\text{Pt}(o\text{-S}_2\text{C}_6\text{F}_4)(\text{dhpp})]$  (**4f**) and the trinuclear complex  $[\text{Pt}_3(\mu_3\text{-S})_2(\text{dhpp})_3]^{+2}$  (**T**), which models **II** and **III**, respectively. This step was calculated by considering the reaction  $\text{3f} + \text{1} \rightarrow \text{4f} + \text{T}$ , and the distances and angles obtained by **4f** were compared with those coming from the crystal structure of **II**. As shown in Fig. 3, the optimized geometry fits well the crystallographic structure. Considering the energy of this step, the fragmentation is strongly exothermic as it requires  $99.6 \text{ kJ mol}^{-1}$ .

Overall, the mechanism of this reaction can be described as a double aromatic nucleophilic substitution ( $\text{S}_{\text{N}}\text{Ar}$ ). This mechanism is usually believed to follow a two-step process: addition of the nucleophile to the aromatic ring, forming the so called Meisenheimer intermediate, and elimination of the leaving group.<sup>40</sup> However in this case the Meisenheimer complex is not a real intermediate; instead, it is the transition state. Such behaviour has already been found in theoretical studies of nucleophilic aromatic substitutions.<sup>41–43</sup> This reaction requires time (5 days) and temperature ( $110.6 \text{ }^\circ\text{C}$ ) to evolve **1** + pfb into  $[\text{Pt}(o\text{-S}_2\text{C}_6\text{F}_4)(\text{dppp})]$  (**II**). The high energy barriers obtained ( $131.7 \text{ kJ mol}^{-1}$  and  $137.1 \text{ kJ mol}^{-1}$  for the first and second C–F nucleophilic substitutions, respectively) agree with these hard conditions. The fragmentation of the product obtained through these steps, modelled by **3f**, results in formation of **II** and  $[\text{Pt}_3(\mu_3\text{-S})_2(\text{dppp})_3]^{+2}(\text{F})_2$  (**III-F**<sub>2</sub>). Considering that the overall observed reaction is very slow (5 days at  $110 \text{ }^\circ\text{C}$ ) it is reasonable to consider that the fragment  $[\text{Pt}(\text{dppp})]^{+2}$  formed by the fragmentation of **3f** reacts with unreacted **I** to afford **III-F**<sub>2</sub> as the final product.

### Single C–F bond activation in perfluoropyridine

**Experimental study.** Addition of an excess of perfluoropyridine to a solution of  $[\text{Pt}_2(\mu\text{-S})_2(\text{dppp})_2]$  in toluene at  $0 \text{ }^\circ\text{C}$  yielded after 15 min a yellow solid, which was isolated by filtration. This solid (**IV-F**) was firstly characterised by  $^{19}\text{F}$  NMR in  $d_6$ -DMSO, where two signals were observed, at  $\delta -94.9$  and  $-127.4$  ppm, consistently with the substitution in pfp of the fluorine atom in

the *para* position to the nitrogen. The spectrum also exhibited a broad signal at  $\delta -148.8$ , which is within the expected chemical shift range for fluoride ions forming hydrogen bonds in species such as  $[\text{F}_2\text{H}]^-$  or  $[(\text{FH})_n\text{F}]^-$ .<sup>34,44–46</sup> The disappearance of this broad signal when the anion in **IV-F** was replaced by  $\text{ClO}_4^-$  confirmed the proposed C–F bond activation in the perfluoropyridine molecule (Scheme 3).



**Scheme 3** Reaction between [Pt<sub>2</sub>(μ-S)<sub>2</sub>(dppp)<sub>2</sub>] (**I**) and perfluoropyridine (pfp)

The <sup>31</sup>P{<sup>1</sup>H} NMR spectra of **IV-F** showed two signals with the same multiplicity and intensity, and both with two satellites ( $\delta = 2.4$  ppm,  $J_{\text{Pt-P}}^1 = 3412$  Hz;  $\delta = 1.6$  ppm,  $J_{\text{Pt-P}}^1 = 2567$  Hz). This is indicative of the presence of two nonequivalent pairs of phosphorus in [Pt<sub>2</sub>(μ-S){μ-(*p*-SC<sub>5</sub>F<sub>4</sub>N)}(dppp)<sub>2</sub>]<sup>+</sup>, one pair *trans* to the thiolate bridge and the other pair *trans* to the sulfide bridge. The ESI-MS spectrum, which showed a major peak at  $m/z = 1428.4$  Da is also in good agreement with the expected theoretical value for **IV** cation (1428.2 Da).

X-Ray quality crystals were obtained by slow evaporation from methanol solution. The structure of the dinuclear [Pt<sub>2</sub>(μ-S){μ-(*p*-SC<sub>5</sub>F<sub>4</sub>N)}(dppp)<sub>2</sub>]<sup>+</sup> (**IV**) cation was unequivocally determined. However, disordered distribution of anions and solvent molecules hampered the modelling of their position. Selected angles and distances in **IV** are given in Table 2. The structure of the cations consists of a hinged central Pt<sub>2</sub>(μ-S)(μ-SR) ring fused to two Pt<sub>2</sub>P<sub>2</sub>C<sub>3</sub> rings (Fig. 4). The dihedral angle between the two PtSS' planes is 132.7°. With the thiolate group in *endo* position with respect to the {Pt<sub>2</sub>SS'} ring. Unlike **IV**, the R group is in *exo* position in a closely related complex containing the {Pt<sub>2</sub>(μ-S)(μ-SR)} core, with R = CH<sub>3</sub>.<sup>28</sup> Thus, while in the *exo* structure the SSC

**Table 2** Selected bond lengths (Å) and angles (°) for cation **IV**

<b>IV</b>			
Bond lengths/Å			
Pt(1)–S(1)	2.320(2)	Pt(2)–S(2)	2.390(2)
Pt(1)–S(2)	2.373(2)	Pt(2)–P(1)	2.298(2)
Pt(1)–P(3)	2.285(2)	Pt(2)–P(2)	2.249(2)
Pt(1)–P(4)	2.254(2)	S(2)–C(1)	1.773(9)
Pt(2)–S(1)	2.333(2)		
Bond angles/°			
S(1)–Pt(1)–S(2)	77.03(8)	S(1)–Pt(2)–P(2)	89.05(8)
S(1)–Pt(1)–P(3)	174.39(8)	S(2)–Pt(2)–P(1)	101.96(8)
S(1)–Pt(1)–P(4)	88.89(8)	S(2)–Pt(2)–P(2)	165.11(8)
S(2)–Pt(1)–P(3)	102.62(8)	P(1)–Pt(2)–P(2)	92.87(9)
S(2)–Pt(1)–P(4)	163.63(8)	Pt(1)–S(1)–Pt(2)	93.21(8)
P(3)–Pt(1)–P(4)	92.20(8)	Pt(1)–S(2)–Pt(2)	90.46(8)
S(1)–Pt(2)–S(2)	76.46(1)	Pt(1)–S(2)–C(1)	115.6(3)
S(1)–Pt(2)–P(1)	171.62(8)	Pt(2)–S(2)–C(1)	110.4(3)

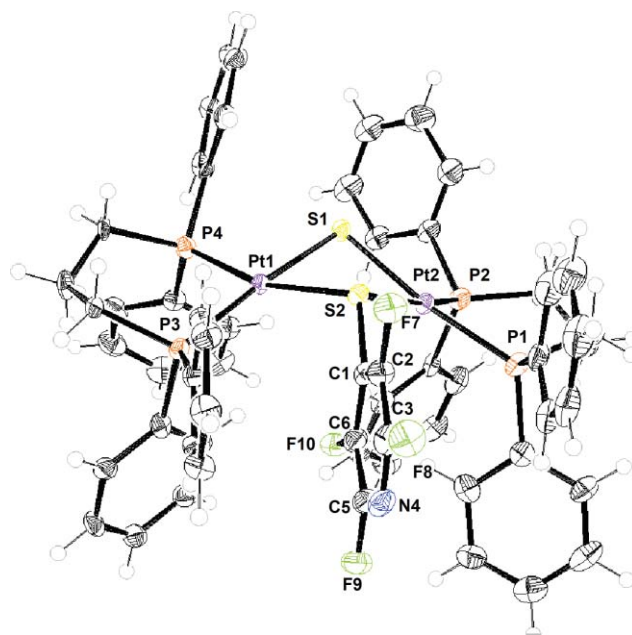


**Fig. 4** Displacement ellipsoid plot (20% probability) of [Pt<sub>2</sub>(μ-S){μ-(*p*-SC<sub>5</sub>F<sub>4</sub>N)}(dppp)<sub>2</sub>]<sup>+</sup> (**IV**). H atoms omitted.

angle is 85.1°, in **IV** this angle is 210.6°. The origin of the preference for the *endo* isomer in **IV** could be the stabilizing interactions between the {SC<sub>5</sub>F<sub>4</sub>N} fragment and the phenyl groups of the dppp ligand. The *endo* geometry allows π–π stacking interactions between the aromatic C<sub>5</sub>F<sub>4</sub>N ring and two phenyl groups, each one from a different phosphine ligand. In addition, the fluorine atoms of the pfp could establish C–F⋯H–C interactions with the phenyl hydrogens.

**Theoretical study.** The computational study of the reaction of [Pt(μ-S)<sub>2</sub>(dhpp)<sub>2</sub>] (**1**) with perfluoropyridine (pfp) has been performed. In contrast to pfb, this substrate has three different positions susceptible of fluoride substitution: *ortho*, *meta* and *para*. Giving the preference of *ortho* and *para* positions for nucleophilic substitution,<sup>9,47</sup> only the reactions in these two positions have been considered. The energy profiles obtained for both reactions are depicted in Fig. 5. Similarly to pfb, the reaction of **1** with pfp initiates with the nucleophilic substitution of the fluoride in *para* position through **TS1n**, with an energy barrier of 85.9 kJ mol<sup>-1</sup>. The analogous reaction but replacing the fluoride in *ortho* position has a barrier 32.8 kJ mol<sup>-1</sup> higher in energy (**TS3n**). This energy difference accounts for the C–F bond activation taking place only in *para* position. In addition, this position is not only the most preferred kinetically, but also thermodynamically. Thus, the product **1n** (3.7 kJ mol<sup>-1</sup>) is more stable than **4n** (31.9 kJ mol<sup>-1</sup>) (Fig. 5). The geometries of **TS1n** and **1n** are similar to those of the related species in the reaction with pfb, **TS1f** and **1f**, respectively. In **TS1n** the {Pt<sub>2</sub>S<sub>2</sub>} core has a dihedral angle of 166.4° and an SCF angle of 95.3° (Fig. 6). The S⋯C and C⋯F distances are 1.894 Å and 1.683 Å, shorter and longer, respectively, than in **TS1f**, showing a more advanced transition state.

In order to analyse why the second fluoride substitution does not take place with perfluoropyridine, the computational study of this step has been also pursued. Only the reaction starting from intermediate **1n**, which is the most favoured kinetically

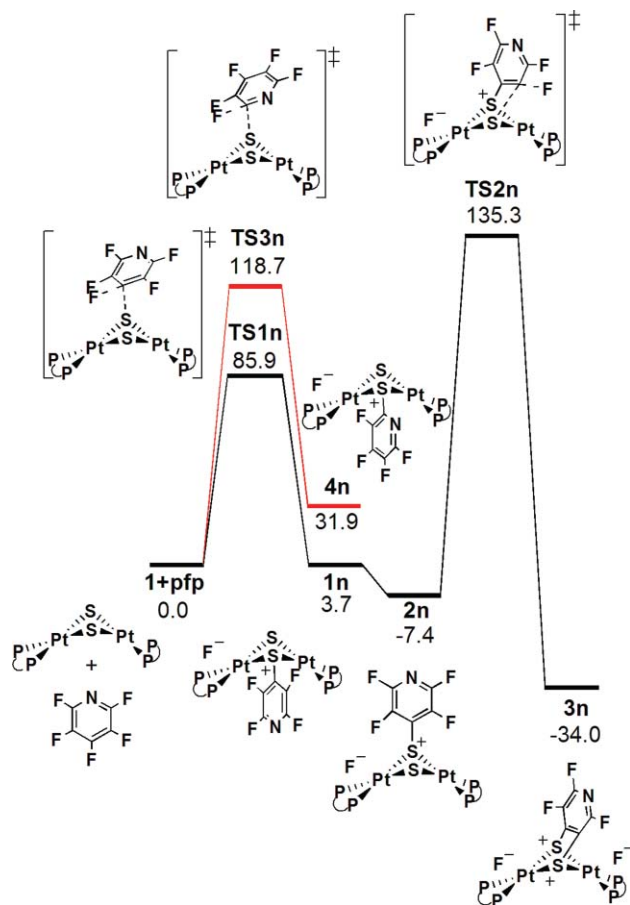


**Fig. 5** Energy profile in toluene of the C–F bond activation mechanism of perfluoropyridine (pfp) by  $[\text{Pt}_2\text{S}_2(\text{dhpp})]$  (**1**). All energies in  $\text{kJ mol}^{-1}$ .

and thermodynamically, and also the only one experimentally observed, has been considered. This intermediate requires a previous endo–exo isomerization process to enable the second fluoride substitution. From the exo intermediate (**2n**,  $11.1 \text{ kJ mol}^{-1}$  below **1n**) the sulfide bridge can attack only a carbon in *ortho* position related to sulfide ligand (*meta* related to nitrogen). The energy barrier of this second substitution is  $142.7 \text{ kJ mol}^{-1}$  (**TS2n**), much higher than the first substitution ( $85.9 \text{ kJ mol}^{-1}$ ). In this transition state, the  $\text{S} \cdots \text{C}$  and  $\text{C} \cdots \text{F}$  distances are  $2.060 \text{ \AA}$  and  $1.597 \text{ \AA}$ , respectively (Fig. 6). Remarkably, in all transition states (with pfp and pfb), the energy barrier increases with longer  $\text{C} \cdots \text{S}$  distances. The final product of the double fluoride substitution is complex **3n**,  $34.0 \text{ kJ mol}^{-1}$  more stable than reactants. In this case, the reaction of  $3\mathbf{n} + \mathbf{1} \rightarrow 5\mathbf{n} + \mathbf{T}$  (where  $5\mathbf{n} = [(\text{dhpp})\text{Pt}(\text{S}_2\text{C}_6\text{F}_4)]$ ) is also exothermic by  $107.5 \text{ kJ mol}^{-1}$ .

These theoretical results are in agreement with the experimental observations for the reaction of **1** with pfp. Thus, this reaction is fast and requires low temperature ( $15 \text{ min}$  at  $0 \text{ }^\circ\text{C}$ ) to afford  $[\text{Pt}_2(\mu\text{-S})\{\mu\text{-}(p\text{-SC}_5\text{F}_4\text{N})\}(\text{dppp})_2]\text{F}$  (**IV-F**). The energy barrier for the first fluoride substitution ( $85.9 \text{ kJ mol}^{-1}$ ) is significantly lower than that for the reaction with pfb ( $131.7 \text{ kJ mol}^{-1}$ ); this can explain the different experimental conditions required in these two reactions. This difference between the energy barrier of pfb and pfp in the first fluoride substitution is not observed for the second substitution. Thus, the energy barrier to activate the second C–F bond in perfluoropyridine is  $142.7 \text{ kJ mol}^{-1}$  (**TS2n**), similar

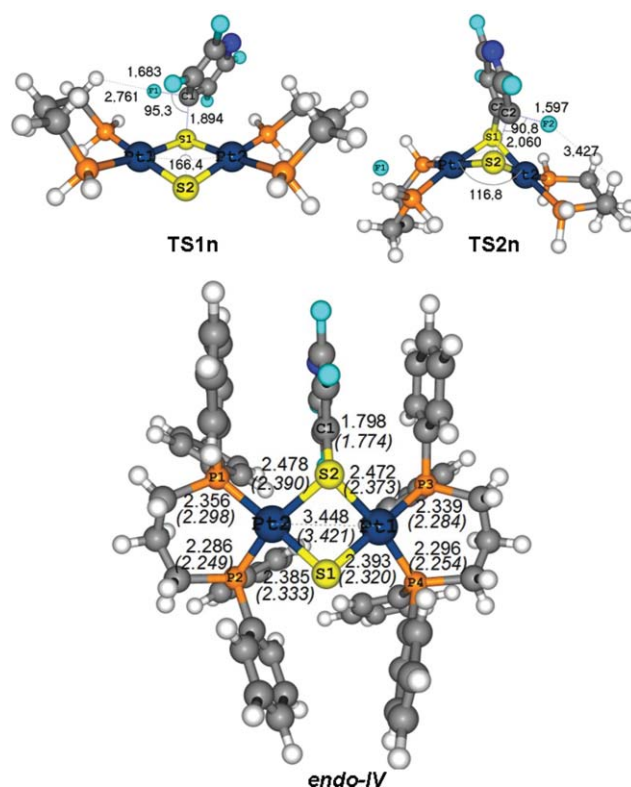


**Fig. 6** Optimized geometries of transition states (**TS1n** and **TS2n**) and complex **endo-IV** with the most representative distances ( $\text{\AA}$ ) for this structure and for the crystal structure of **IV** (numbers in italics).

to that obtained in pfb ( $137.1 \text{ kJ mol}^{-1}$ ). This energy barrier is not feasible at  $0 \text{ }^\circ\text{C}$  and consequently the reaction stops before reaching this stage. At higher temperatures the reaction gives a mixture of platinum complexes that have not been characterized. Probably, the absence of **1** in solution, which reacts quickly with pfp, impairs the formation of  $[\text{Pt}_3(\mu_3\text{-S})_2(\text{dppp})_3]^{2+}$ , thus directing the system towards several other by-products resulting from the cleavage of the  $\{\text{Pt}_2\text{S}_2\}$  core.

**Endo–exo exchange in cation IV.** As it has been described in the experimental section, **IV** crystallizes with the R group of the  $\{\text{Pt}_2(\mu\text{-S})(\mu\text{-SR})\}$  core in endo position. The stabilization of this conformer comes from the interaction between the  $\{\text{SC}_5\text{F}_4\text{N}\}$  fragment and the phenyl groups of the dppp ligand. Thus, the model system used to study the reaction mechanism, in which the Ph groups in dppp have been replaced by H, can not reproduce this interaction. Consequently, the exo isomer **2n** is more stable than the endo **1n** by  $11.1 \text{ kJ mol}^{-1}$  (Fig. 5). To estimate the importance of this interaction, the dynamic process endo–exo arising from the flexibility of the  $\{\text{Pt}(\mu\text{-S})(\mu\text{-SR})\text{Pt}\}$  has been studied for cation **IV** considering the full system, including the phenyl rings in the theoretical calculation (Fig. 6 and 7). This study has been performed using a hybrid QM/MM method (see Computational details). The analogous system used in the mechanistic study was described at the quantum mechanics (QM) level, whereas the phenyl groups were described at the molecular mechanics (MM) level.

Considering the full system for complexes **1n** and **2n**, there is a change in the relative stability of these complexes, the endo isomer

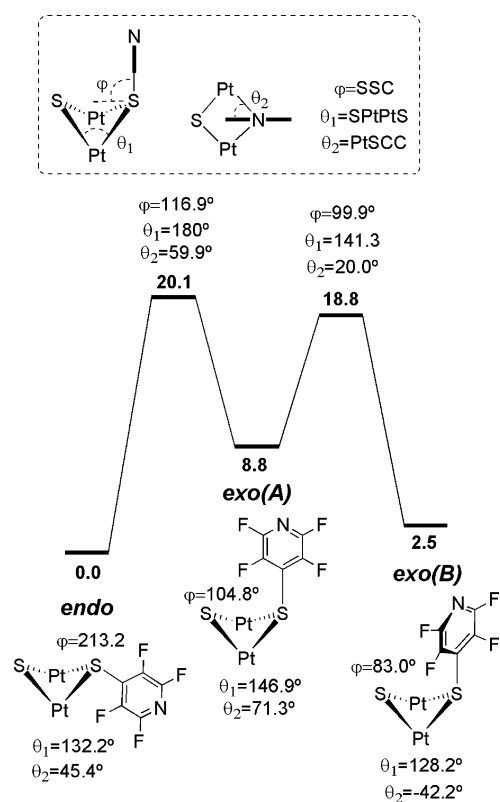


**Fig. 7** Energy profile in the gas phase of the endo–exo dynamic process arising from the flexibility of the {Pt( $\mu$ -S)( $\mu$ -SR)Pt} core in **IV**. All energies in  $\text{kJ mol}^{-1}$ .

becoming more stable than the exo one, as it was expected from the X-ray conformation of **IV**. In addition, a new isomer with the fluoropyridyl substituent in the exo position has been found as an energy minimum.

The structural difference between the two exo isomers, exo(A) and exo(B) in Fig. 7, arises from the relative position of the fluoropyridine ring relative to the SSC plane, almost parallel in exo(A) (PtSCC dihedral angle ( $\theta_2$ ) of  $71.3^\circ$ ), and almost perpendicular in exo(B) ( $\theta_2 = -42.2^\circ$ ). Exo(B) isomer is only slightly less stable than endo ( $2.5 \text{ kJ mol}^{-1}$ ), exo(A) being placed  $6.3 \text{ kJ mol}^{-1}$  above exo(B). Exo(A) may be obtained from the endo isomer by the hinging motion of the {Pt $_2$ S $_2$ } core, while exo(B) implies the rotation of the ring around the S–C  $\sigma$ -bond. The energy barriers for these transformations have been estimated considering in each case the corresponding reaction coordinate:  $\theta_1$  from endo to exo(A) and  $\theta_2$  from exo(A) to exo(B), obtaining values around  $20 \text{ kJ mol}^{-1}$ , which point out a fast interconversion between the different isomers.

With these results, a dynamic endo–exo process is expected at room temperature. This is in good agreement with the  $^{19}\text{F}$  NMR data. While at room temperature only two signals at  $\delta -94.9$  and  $-127.4 \text{ ppm}$  are observed, it is necessary to go down to  $-90^\circ\text{C}$ , as shown in Fig. 8, to separate the signals corresponding to two different isomers of **IV**. These two isomers appear in almost the same proportion, indicating a very close thermodynamic stability. Thus, the signals observed at  $-90^\circ\text{C}$  ( $\delta = -94.2, -94.8, -125.7, -128.2 \text{ ppm}$ ) probably correspond to the endo and the most stable exo (*i.e.* exo(B)) isomers.

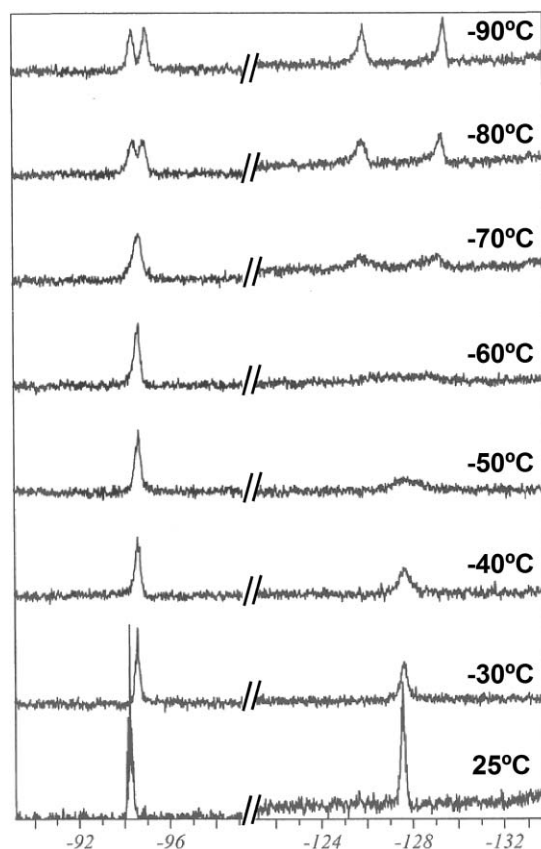


**Fig. 8** VT- $^{19}\text{F}$  NMR spectrum of  $[\text{Pt}_2(\mu\text{-S})\{\mu\text{-}(p\text{-SC}_5\text{F}_4\text{N})\}(\text{dppp})_2]\text{F}$  (**IV-F**).

## Experimental

### Materials and methods

All the manipulations were carried out at room temperature under an atmosphere of pure dinitrogen, and conventionally dried and degassed solvents were used throughout. These were Purex Analytical Grade from SDS. The synthesis of  $[\text{Pt}_2(\mu\text{-S})_2(\text{dppp})_2]$  (**I**) has already been reported.<sup>26</sup> Perfluorobenzene and perfluoropyridine reagents were purchased from Aldrich in their purest presentation ( $>99.5\%$ ). The purity of these reagents was examined by  $^{19}\text{F}$ -NMR, observing that no signals other than those corresponding to the reagent itself could be detected.

Elemental analyses were performed on a Carlo-Erba CHNS EA-1108 analyzer. The ESI-MS and FAB-MS measurements were performed on a VG Quattro Micromass Instrument by using 1 : 1 acetonitrile–water as carrier (ESI-MS) or 3-nitrobenzil alcohol (NBA) as matrix in the positive ion mode (FAB-MS).  $^{31}\text{P}\{^1\text{H}\}$ ,  $^{19}\text{F}$  NMR spectra were recorded from samples in  $d_6$ -DMSO solution at room temperature using a Bruker AC250 spectrometer.  $^1\text{H}$  and  $^{13}\text{C}$  chemical shift are relative to  $\text{SiMe}_4$ .  $^{19}\text{F}$  chemical shift is relative to  $\text{CFCl}_3$  and  $^{31}\text{P}\{\text{H}\}$  NMR spectra were referenced to external  $85\% \text{H}_3\text{PO}_4$ .

### Synthesis of $[\text{Pt}(\text{dppp})(o\text{-S}_2\text{C}_6\text{F}_4)]$ (**II**)

Perfluorobenzene (1 mL, 8.7 mmol) was added to a solution of  $[\text{Pt}_2(\mu\text{-S})_2(\text{dppp})_2]$  (340 mg, 0.3 mmol) (**I**) in dry toluene (30 mL). The reaction mixture was stirred at reflux ( $111^\circ\text{C}$ ) and after

5 days it was filtered. The toluene solution was evaporated to dryness under vacuum. The remaining yellow solid was washed with ether. From this solid, X-ray quality crystals were obtained by slow evaporation from an acetone DMSO mixture solution. Yield: 42 mg (39%). Anal. calcd for  $C_{33}F_4H_{26}P_2PtS_2$  (819): C 48.35, H 3.20, S 7.82. Found: C 48.31, H 3.52, S 7.42.

### Synthesis of $[Pt_2(dppp)_2(\mu-S)\{\mu-(p-SC_5F_4N)\}]F$ (IV)

Perfluoropyridine (0.84 mL, 7.65 mmol) was added to a solution of  $[Pt_2(\mu-S)_2(dppp)_2]$  (98 mg, 0.08 mmol) in dry toluene (15 mL). After 15 min, a pale yellow solid appeared. The solid product was collected by filtration, washed with toluene, and dried with diethyl ether. Yield: 48 mg (43%). X-Ray quality crystals were obtained by slow evaporation of a  $CH_2Cl_2$  solution. Anal. calcd for  $C_{59}F_5NH_{52}P_4Pt_2S_2 \cdot H_2O \cdot CH_2Cl_2$  (1551.17): C 46.46, H 3.64, N 0.90. Found: C 46.37, H 3.54, N 0.88.

### X-Ray crystallographic characterization†

A summary of crystal data, data collection, and refinement parameters for the structural analysis of complexes **II** and **IV-F** is given in Table 3. Measurements of diffraction intensity data were collected respectively on a Bruker SMART CCD-1000 and APPEX-II CCD area-detector diffractometer with graphite-monochromated Mo  $K\alpha$  radiation ( $\lambda = 0.71073 \text{ \AA}$ ). Absorption correction was carried out by semiempirical methods based on redundant and symmetry-equivalent reflections with the aid of the SADABS program.<sup>48</sup> The structure was resolved by direct methods (DIRDIF<sup>49</sup> and SIR97<sup>50</sup>) and refined by full-matrix least-squares based on  $F^2$ , with the aid of SHELX-97<sup>51</sup> software. All hydrogen atoms were included at geometrically calculated positions with thermal parameters derived from the parent atoms. In compound **IV-F** the best crystal found only diffracts up to  $0.95 \text{ \AA}$  resolution at  $22.02^\circ$  in theta, Mo  $K\alpha$ , and thus, data were only collected out to  $22^\circ$ . The solvent and fluoride anion molecules appear to be highly disordered thus making it difficult to model its position and distribution reliably. Attempts to solve and refine

the crystal structure in lower symmetry space groups do not solve the disorder problem. There were very high correlations among symmetry related geometrical parameters in the highest symmetry space group ( $P2_1/n$ ). The electron density maxima found inside the voids were equally unexplainable by means of reasonable molecular models. Therefore, the SQUEEZE<sup>52,53</sup> function was used to eliminate the contribution of the electron density in the disordered solvent region from the measured intensity data (two  $690 \text{ \AA}^3$  voids per unit cell containing 319 electrons each) and therefore the solvent-free data was employed in the final refinement. The method to determine the number of electrons per void is the previously reported as the 'BYPASS' procedure,<sup>52</sup> implemented in the PLATON software as SQUEEZE calculation. The lack of high resolution data (lower data/parameter ratio) and the use of the SQUEEZE procedure to account for the high level of disorder inside the voids caused problems in the least-square refinement (mainly in the  $U_{ij}$  behaviour). To minimize this effect the structure was submitted to further refinement cycles including a complete set of geometrical restraints (a mixture of SIMU and ISOR instructions). The high number of restraints finally used (696) significantly improved the anisotropic atomic displacement parameters obtained from the initial refinement (12 restraints). Molecular graphics are represented by Ortep-3 for Windows.

### Computational details

This study was made using two different models: one small, where all phenyl substituents of the phosphine ligands were replaced by H; and one complete, where the full system was considered. The calculations for the small system were performed using the Gaussian03 package.<sup>54</sup> In this case, the geometries of the minima and transition states were fully optimized, without any symmetry restriction. Frequency calculations were performed to characterize the stationary points as minima or transition states. Single point calculations including solvent effects were performed at the optimized gas-phase geometries, using the CPCM approach,<sup>55,56</sup> which is an implementation of the conductor-like screening solvation model (COSMO) in Gaussian03. Toluene, the solvent used in all experiments, was chosen as solvent (dielectric constant  $\epsilon = 2.379$ ).

QM/MM IMOMM calculations<sup>57</sup> for the complete system were performed with a program build from modified version of two standard programs: Gaussian98 for the quantum mechanics part<sup>58</sup> and mm3(92) for the molecular mechanics part.<sup>59</sup> The QM region was  $[Pt(\mu-S)_2(dhpp)_2]$  plus perfluorobenzene and perfluoropyridine. The phenyl groups of the phosphine were computed at the MM level. Optimizations were full except for the connection between the QM and the MM region where P–H distance was fixed to  $1.420 \text{ \AA}$ .

Quantum calculations in the small and complete systems were performed at the B3LYP level.<sup>60,61</sup> For the Pt, P and S atoms, the lanl2dz effective core potential was used to describe the innermost electrons,<sup>62</sup> whereas their associated double- $\zeta$  basis set was employed for the rest of the electrons. An extra series of d-polarization functions were also added for P (exp. 0.387) and S (exp. 0.503) atoms.<sup>63</sup> The carbon and nitrogen atoms of perfluorobenzene and perfluoropyridine were described by the 6–31G(d) basis set.<sup>64</sup> The rest of the C and H atoms were described by the 6–31G basis set. The fluorine atoms were described by the 6–31G+(d) basis set.<sup>65</sup>

**Table 3** Crystallographic data for complexes **II** and **IV**

	<b>II</b>	<b>IV</b>
Formula	$C_{33}H_{26}S_2P_2F_4Pt$	$C_{59}H_{52}F_4NP_4Pt_2S_2$
$M_r$	819.69	1429.2
Crystal system	Monoclinic	Monoclinic
Space group	$P2_1/c$	$P2_1/n$
$a/\text{\AA}$	13.393(4)	12.7777(5)
$b/\text{\AA}$	21.653(6)	19.9091(6)
$c/\text{\AA}$	12.975(3)	24.4992(9)
$\alpha/^\circ$	90	90
$\beta/^\circ$	113.829(4)	95.906(2)
$\gamma/^\circ$	90	90
$V/\text{\AA}^3$	3442.0(16)	6199.3(4)
$T/K$	120.0(1)	100.0(1)
$Z$	4	4
$\rho_{\text{calcd}}/\text{g cm}^{-3}$	1.582	1.531
$\mu/\text{mm}^{-1}$	4.33	4.73
Reflections collected	28 890	69 141
Unique reflections ( $R_{\text{int}}$ )	7064(0.0614)	7575(0.126)
Parameters/restraints	379/0	649/696
Goodness-of-fit on $F^2$	1.398	0.928
$R_1, wR_2 [I > 2\sigma(I)]$	0.0341, 0.0784	0.0369, 0.0771
$R_1, wR_2$ (all data)	0.0548, 0.0847	0.0596, 0.0821

The MM calculations in the full system were carried out with the MM3 force field.<sup>66</sup> The van der Waals parameters for platinum were taken from UFF force field.<sup>67</sup> Torsional contributions involving dihedral angles with the metal atom in terminal position were set to zero.

## Conclusions

In the present work the C–F bond activation of aromatic compounds (perfluorobenzene and perfluoropyridine) has been achieved by the  $[\text{Pt}_2(\mu\text{-S})_2(\text{dppp})_2]$  complex. Recently, the same complex has been used to activate the aliphatic substrate 1,3-difluoro-2-propanol (Scheme 1).<sup>34</sup> These two examples show the efficiency of  $[\text{Pt}_2(\mu\text{-S})_2(\text{dppp})_2]$  to activate C–F bonds of organic substrates by nucleophilic substitution. In the case of 1,3-difluoro-2-propanol, the computational study of the reaction mechanism revealed an important effect of the OH group assisting the fluorine departure in a  $\text{S}_{\text{N}}2$  process. In the case of perfluoropyridine and perfluorobenzene, this requirement is not necessary and consequently the C–F bond activation in aromatic compounds seems to be more general. The theoretical study has revealed that the reaction proceeds through a  $\text{S}_{\text{N}}\text{Ar}$  mechanism, accounting for the different experimental condition required in each reaction and for the various products obtained. According to these results the different reactivity of perfluorobenzene and perfluoropyridine towards **I** resides in the kinetics of these reactions, their thermodynamics being quite similar. The products of the first substitution (**2f** and **2n**) are few  $\text{kJ mol}^{-1}$  below reactants ( $-4.3$  and  $-7.4$   $\text{kJ mol}^{-1}$ , respectively) and the products of the second substitutions are around 35  $\text{kJ mol}^{-1}$  below in the two cases. On the contrary, the energy barriers for the first C–F substitution are remarkably different: 131.7  $\text{kJ mol}^{-1}$  with perfluorobenzene and 85.9  $\text{kJ mol}^{-1}$  with perfluoropyridine.

C–F bond activation in both organic substrates is also selective. With perfluorobenzene the double C–F bond activation takes place in *ortho* position. This is the only possibility considering the disposition of the two sulfur atoms in complex **I**. This orientation is not usual in reactions with thiolates where the substitution of two fluorides is always in positions 1,4.<sup>10</sup> In the case of perfluoropyridine, the activation in *para* position with respect to nitrogen is more common.<sup>9</sup> As it has been shown in this study, the reason in this case is not only kinetic but also thermodynamic being **In** 28.2  $\text{kJ mol}^{-1}$  more stable than **4n**.

## Acknowledgements

We are grateful to Dr A. L. Llamas and Dr B. Dacuña (Unidade de Raios X RIAIDT, Universidade de Santiago de Compostela, Spain) for crystal structure determinations. The authors thank the financial support from the “Ministerio de Ciencia e Innovación” of Spain (projects CTQ2004-01463, CTQ2008-06866-C02-01/BQU and Consolider Ingenio 2010 CSD2007-00006). R. M. B. thanks the Spanish MICINN for funding through the “Ramón y Cajal” program. The use of the computational facilities of the “Centre de Supercomputació de Catalunya” is greatly appreciated.

## References

1 D. M. Lemal, *J. Org. Chem.*, 2004, **69**, 1.

- 2 *Organofluorine Chemistry: Principles and Commercial Applications*, ed. R. E. Banks, B. E. Smart and J. C. Tatlow, Plenum, New York, 1994.
- 3 J. Burdeniuc, B. Jedlicka and R. H. Crabtree, *Chem. Ber.*, 1997, **130**, 145.
- 4 J. L. Kiplinger, T. G. Richmond and C. E. Osterberg, *Chem. Rev.*, 1994, **94**, 373.
- 5 W. D. Jones, *Dalton Trans.*, 2003, 3991.
- 6 U. Mazurek and H. Schwarz, *Chem. Commun.*, 2003, 1321.
- 7 T. Braun and R. N. Perutz, *Chem. Commun.*, 2002, 2749.
- 8 H. Torrens, *Coord. Chem. Rev.*, 2005, **249**, 1957.
- 9 G. M. Brooke, *J. Fluorine Chem.*, 1997, **86**, 1.
- 10 *Organo-Fluorine Compounds*, ed. B. Baasner, H. Hagemann and J. C. Tatlow, Stuttgart, New York, 4th edn, 2000, E 10b/Part 2, 880.
- 11 M. Aizenberg and D. Milstein, *Science*, 1994, **265**, 359.
- 12 A. Steffen, M. I. Sladek, T. Braun, B. Neumann and H. G. Stammer, *Organometallics*, 2005, **24**, 4057.
- 13 T. Schaub, M. Backes and U. Radius, *J. Am. Chem. Soc.*, 2006, **128**, 15964.
- 14 T. Braun, F. Wehmeier and K. Altenhoner, *Angew. Chem., Int. Ed.*, 2007, **46**, 5321.
- 15 R. Bosque, E. Clot, S. Fantacci, F. Maseras, O. Eisenstein, R. N. Perutz, K. B. Renkema and K. G. Caulton, *J. Am. Chem. Soc.*, 1998, **120**, 12634.
- 16 M. Reinhold, J. E. McGrady and R. N. Perutz, *J. Am. Chem. Soc.*, 2004, **126**, 5268.
- 17 S. Park, M. Pontierjohnson and D. M. Roundhill, *J. Am. Chem. Soc.*, 1989, **111**, 3101.
- 18 R. P. Hughes, D. C. Lindner, A. L. Rheingold and L. M. LiableSands, *J. Am. Chem. Soc.*, 1997, **119**, 11544.
- 19 R. P. Hughes, R. B. Laritchev, A. Williamson, C. D. Incarvito, L. N. Zakharov and A. L. Rheingold, *Organometallics*, 2002, **21**, 4873.
- 20 P. L. Shutov, S. S. Karlov, K. Harms, D. A. Tyurin, J. Sundermeyer, J. Lorberth and G. S. Zaitseva, *Eur. J. Inorg. Chem.*, 2004, 2498.
- 21 S. A. Macgregor, *Chem. Soc. Rev.*, 2007, **36**, 67.
- 22 A. Nova, S. Erhardt, N. A. Jasim, R. N. Perutz, S. A. Macgregor, J. E. McGrady and A. C. Whitwood, *J. Am. Chem. Soc.*, 2008, **130**, 15499.
- 23 S. Erhardt and S. A. Macgregor, *J. Am. Chem. Soc.*, 2008, **130**, 15490.
- 24 P. Gonzalez-Duarte, A. Lledos and R. Mas-Balleste, *Eur. J. Inorg. Chem.*, 2004, 3585.
- 25 S. W. A. Fong and T. S. A. Hor, *J. Chem. Soc., Dalton Trans.*, 1999, 639.
- 26 J. Chatt and D. M. P. Mingos, *J. Chem. Soc. A*, 1970, 1243.
- 27 R. Ugo, G. La Monica, S. Cenini, A. Segre and F. Conti, *J. Chem. Soc. A*, 1971, 522.
- 28 C. E. Briant, C. J. Gardner, T. S. A. Hor, N. D. Howells and D. M. P. Mingos, *J. Chem. Soc., Dalton Trans.*, 1984, 2645.
- 29 R. Mas-Balleste, M. Capdevila, P. A. Champkin, W. Clegg, R. A. Coxall, A. Lledos, C. Megret and P. Gonzalez-Duarte, *Inorg. Chem.*, 2002, **41**, 3218.
- 30 S. H. Chong, A. Tjindrawan and T. S. A. Hor, *J. Mol. Catal. A*, 2003, **204**, 267.
- 31 F. Novio, R. Mas-Balleste, I. Gallardo, P. Gonzalez-Duarte, A. Lledos and N. Vila, *Dalton Trans.*, 2005, 2742.
- 32 S. H. Chong, D. J. Young and T. S. A. Hor, *Chem.–Asian J.*, 2007, **2**, 1356.
- 33 A. Nova, P. Gonzalez-Duarte, A. Lledos, R. Mas-Balleste and G. Ujaque, *Inorg. Chim. Acta*, 2006, **359**, 3736.
- 34 A. Nova, R. Mas-Balleste, G. Ujaque, P. Gonzalez-Duarte and A. Lledos, *Chem. Commun.*, 2008, 3130.
- 35 R. Mas-Balleste, G. Aullon, P. A. Champkin, W. Clegg, C. Megret, P. Gonzalez-Duarte and A. Lledos, *Chem.–Eur. J.*, 2003, **9**, 5023.
- 36 M. Arroyo, S. Bernes, J. L. Brioso, E. Mayoral, R. L. Richards, J. Rius and H. Torrens, *J. Organomet. Chem.*, 2000, **599**, 170.
- 37 M. Capdevila, W. Clegg, P. Gonzalez-Duarte, A. Jarid and A. Lledos, *Inorg. Chem.*, 1996, **35**, 490.
- 38 G. Aullon, G. Ujaque, A. Lledos and S. Alvarez, *Chem.–Eur. J.*, 1999, **5**, 1391.
- 39 G. Aullon, G. Ujaque, A. Lledos, S. Alvarez and P. Alemany, *Inorg. Chem.*, 1998, **37**, 804.
- 40 J. Miller, *Aromatic Nucleophilic Substitution*, Elsevier, Amsterdam, The Netherlands, 1968.
- 41 Y. J. Zheng and R. L. Ornstein, *J. Am. Chem. Soc.*, 1997, **119**, 648.
- 42 Z. Wu and R. Glaser, *J. Am. Chem. Soc.*, 2004, **126**, 10632.
- 43 D. Xu, Y. Wei, J. Wu, D. Dunaway-Mariano, H. Guo, Q. Cui and J. Gao, *J. Am. Chem. Soc.*, 2004, **126**, 13649.

- 44 N. S. Golubev, P. M. Tolstoy, S. N. Smirnov, G. S. Denisov and H.-H. Limbach, *J. Mol. Struct.*, 2004, 700.
- 45 I. G. Shenderovich, H. H. Limbach, S. N. Smirnov, P. M. Tolstoy, G. S. Denisov and N. S. Golubev, *Phys. Chem. Chem. Phys.*, 2002, 4, 5488.
- 46 J. Wessel, U. Behrens, E. Lork, T. Borrmann, W. D. Stohrer and R. Mews, *Inorg. Chem.*, 2002, 41, 4715.
- 47 H. Benmansour, R. D. Chambers, P. R. Hoskin and G. Sandford, *J. Fluorine Chem.*, 2001, 112, 133.
- 48 G. M. Sheldrick, *SADABS, Program for area detector adsorption correction*, Institute for Inorganic Chemistry, University of Göttingen, Germany, 1996.
- 49 P. T. Beurskens, G. Admiraal, G. Beurskens, W. P. Bosman, R. d. Gelder, R. Israel, and J. M. Smits, *DIRDIF*, University of Nijmegen, The Netherlands, 1999.
- 50 A. Altomare, M. C. Burla, M. Camalli, G. L. Casciarano, C. Giacovazzo, A. Guagliardi, A. G. G. Moliterni, G. Polidori and R. Spagna, *J. Appl. Crystallogr.*, 1999, 32, 115.
- 51 G. M. Sheldrick, *SHELXL-97, Program for refinement of crystal structures*, University of Göttingen, Germany, 1997; G. M. Sheldrick, *SHELXS-97, Program for solution of crystal structures*, University of Göttingen, Germany, 1997.
- 52 P. van der Sluis and A. L. Spek, *Acta Crystallogr., Sect. A: Fundam. Crystallogr.*, 1990, 46, 194.
- 53 J. Spek, *Appl. Crystallogr.*, 2003, 36, 7.
- 54 M. J. Frisch, G. W. Trucks, H. B. Schlegel, G. E. Scuseria, M. A. Robb, J. R. Cheeseman, J. A. Montgomery, Jr., T. Vreven, K. N. Kudin, J. C. Burant, J. M. Millam, S. S. Iyengar, J. Tomasi, V. Barone, B. Mennucci, M. Cossi, G. Scalmani, N. Rega, G. A. Petersson, H. Nakatsuji, M. Hada, M. Ehara, K. Toyota, R. Fukuda, J. Hasegawa, M. Ishida, T. Nakajima, Y. Honda, O. Kitao, H. Nakai, M. Klene, X. Li, J. E. Knox, H. P. Hratchian, J. B. Cross, V. Bakken, C. Adamo, J. Jaramillo, R. Gomperts, R. E. Stratmann, O. Yazyev, A. J. Austin, R. Cammi, C. Pomelli, J. Ochterski, P. Y. Ayala, K. Morokuma, G. A. Voth, P. Salvador, J. J. Dannenberg, V. G. Zakrzewski, S. Dapprich, A. D. Daniels, M. C. Strain, O. Farkas, D. K. Malick, A. D. Rabuck, K. Raghavachari, J. B. Foresman, J. V. Ortiz, Q. Cui, A. G. Baboul, S. Clifford, J. Cioslowski, B. B. Stefanov, G. Liu, A. Liashenko, P. Piskorz, I. Komaromi, R. L. Martin, D. J. Fox, T. Keith, M. A. Al-Laham, C. Y. Peng, A. Nanayakkara, M. Challacombe, P. M. W. Gill, B. G. Johnson, W. Chen, M. W. Wong, C. Gonzalez and J. A. Pople, *GAUSSIAN03 (Revision C.02)*, Gaussian, Inc., Wallingford, CT, 2004.
- 55 V. Barone and M. Cossi, *J. Phys. Chem. A*, 1998, 102, 1995.
- 56 M. Cossi, G. Scalmani, N. Rega and V. Barone, *J. Comput. Chem.*, 2003, 24, 669.
- 57 F. Maseras and K. Morokuma, *J. Comput. Chem.*, 1995, 16, 1170.
- 58 M. J. Frisch, G. W. Trucks, H. B. Schlegel, G. E. Scuseria, M. A. Robb, J. R. Cheeseman, V. G. Zakrzewski, J. A. J. Montgomery, R. E. Stratmann, J. C. Burant, S. Dapprich, J. M. Millam, A. D. Daniels, K. N. Kudin, M. C. Strain, O. Farkas, J. Tomasi, V. Barone, M. Cossi, R. Cammi, B. Mennucci, C. Pomelli, C. Adamo, S. Clifford, J. Ochterski, G. A. Petersson, P. Y. Ayala, Q. Cui, K. Morokuma, D. K. Malick, A. D. Rabuck, K. Raghavachari, J. B. Foresman, J. Cioslowski, J. V. Ortiz, B. B. Stefanov, G. Liu, A. Liashenko, P. Piskorz, I. Komaromi, R. Gomperts, R. L. Martin, D. J. Fox, T. Keith, M. A. Al-Laham, C. Y. Peng, A. Nanayakkara, C. Gonzalez, M. Challacombe, P. M. W. Gill, B. Johnson, W. Chen, M. W. Wong, J. L. Andres, C. Gonzalez, M. Head-Gordon, E. S. Replogle and J. A. Pople, *Gaussian, Inc.*, Pittsburgh PA, 1998.
- 59 N. L. Allinger, *MM3(92)*, QCPE, Bloomington, IN, 1992.
- 60 A. D. Becke, *J. Chem. Phys.*, 1993, 98, 5648.
- 61 C. Lee, R. G. Parr and W. Yang, *Phys. Rev.*, 1988, 37, B785.
- 62 W. R. Wadt and P. J. Hay, *J. Chem. Phys.*, 1985, 82, 284.
- 63 A. Höllwarth, M. Böhme, S. Dapprich, A. W. Ehlers, A. Gobbi, V. Jonas, K. F. Köhler, R. Stegmann, A. Veldkamp and G. Frenking, *Chem. Phys. Lett.*, 1993, 208, 237.
- 64 W. J. Hehre, R. Ditchfield and J. A. Pople, *J. Phys. Chem. A*, 1972, 56, 2257.
- 65 M. J. Frisch, J. A. Pople and J. S. Binkley, *J. Chem. Phys.*, 1984, 80, 3265.
- 66 N. L. Allinger, Y. H. Yuh and J. H. Lii, *J. Am. Chem. Soc.*, 1989, 111, 8551.
- 67 A. K. Rappe, C. J. Casewit, K. S. Colwell, W. A. Goddard and W. M. Skiff, *J. Am. Chem. Soc.*, 1992, 114, 10024.